INTERNATIONAL JOURNAL OF PHARMACEUTICAL SCIENCES
[ISSN: 0975-4725; CODEN(USA): IJPS00]
Journal Homepage: https://www.ijpsjournal.com

OPEN ACCESS

Research Paper

Synthesis, Characterization, Molecular Docking & Evaluation of Antibacterial Activity of Isoniazid-Pyrazole Hybrid Scaffolds

Amerullah Ansari*, Sarita, Ankit Kumar Verma

Department of Pharmaceutical Chemistry, Sagar Institute of Technology and Management, Department of Pharmacy, Barabanki, U.P.

ARTICLE INFO

Published: 27 June 2026
Keywords:
Isoniazid, Pyrazole, Molecular Docking, Antibacterial Activity, DHFR Inhibitor, Hybrid Scaffolds, Vilsmeier–Haack Reaction, Heterocyclic Compounds.
DOI:
10.5281/zenodo.20958180

ABSTRACT

The study was based on the concept of molecular hybridization, in which the pharmacologically active isoniazid nucleus was integrated with a biologically significant pyrazole moiety to obtain compounds with enhanced antibacterial efficacy. A series of substituted isoniazid–pyrazole derivatives were synthesized through a multistep synthetic route involving condensation of isoniazid with substituted acetophenones followed by cyclization and formylation using the Vilsmeier–Haack reaction.The synthesized compounds were purified by recrystallization and characterized using physicochemical and spectroscopic techniques. Molecular docking studies were performed using AutoDock Vina against bacterial dihydrofolate reductase (DHFR) enzymes of Escherichia coli (PDB ID: 6XG5) and Staphylococcus aureus (PDB ID: 2W9H) to evaluate binding affinity and interaction profiles. The docking results revealed that the synthesized compounds exhibited favorable interaction patterns and stronger binding affinity than the standard drug trimethoprim. Among the synthesized derivatives, methoxy- and methyl-substituted compounds demonstrated superior docking scores due to enhanced H-bonding with active site amino acid residues. The antibacterial activity of the synthesized compounds was evaluated by the agar disk diffusion method against selected bacterial isolates. The compounds exhibited appreciable antibacterial activity.

INTRODUCTION

Despite tremendous progress in medicine, sanitation, and preventive care, infectious illnesses remain a serious global public health concern. These diseases develop when pathogenic microorganisms, including bacteria, viruses, fungi, and parasites, enter the human body, proliferate, and interfere with regular physiological processes. The severity of infectious

***Corresponding Author:** Amerullah Ansari
Address: *Department of Pharmaceutical Chemistry, Sagar Institute of Technology and Management, Department of Pharmacy, Barabanki, U.P.*
Email ✉: amerullahansari53865@gmail.com
Relevant conflicts of interest/financial disclosures: The authors declare that the research was conducted in the absence of any commercial or financial relationships that could be construed as a potential conflict of interest.

diseases varies greatly, from self-limiting ailments to potentially fatal systemic infections. Beyond personal health, they have an impact on global mortality trends, healthcare spending, and socioeconomic growth.

Infectious diseases continue to rank among the world's leading causes of mortality, especially in low- and middle-income nations, according to data issued by the World Health Organization (WHO). Millions of people die each year from lower respiratory tract infections, diarrhoeal illnesses, TB, and other vector-borne illnesses, according to the WHO. Vaccination, better cleanliness, and efficient antimicrobial therapy have reduced the burden of some diseases, but novel pathogens, antibiotic resistance, and changes in disease transmission brought on by climate change still offer serious risks. The persistence of infectious diseases highlights the ongoing need for surveillance, early diagnosis, and development of new therapeutic strategies.[1]

Global Burden of Infectious Diseases

The worldwide burden of infectious diseases is influenced by a number of factors, including socioeconomic inequality, environmental conditions, healthcare accessibility, and population density. According to WHO estimates, infectious illnesses remain a leading cause of morbidity and mortality globally, especially in places with poor healthcare systems.

Heterocyclic Scaffolds in Medicinal Chemistry

One of the most important types of organic molecules utilised in contemporary drug research and development are heterocyclic compounds. A ring structure with at least one atom other than carbon—typically nitrogen, oxygen, or sulfur—is referred to as a heterocycle. These heteroatoms give heterocycles unique chemical, electrical, and biological properties that make them extremely adaptable pharmacophores. Their extensive use in medicinal chemistry is a result of their capacity to coordinate with biological targets, engage in hydrogen bonding, and exhibit a variety of three-dimensional conformations.

Importance of Heterocycles in Drug Design

Because heterocycles can improve biological activity, molecular recognition, and therapeutic results, they are essential to current drug design. Compounds can engage in hydrogen bonding, metal coordination, and electrostatic interactions with biological targets including enzymes, receptors, and nucleic acids when they contain heteroatoms like nitrogen, oxygen, or sulphur. Drug candidates' binding affinity, potency, and selectivity are all enhanced by these interactions.[25] Furthermore, physicochemical characteristics like solubility, lipophilicity, acidity or basicity, and membrane permeability—all crucial for attaining ideal pharmacokinetic profiles and preserving a balance between stability and bioavailability—can be greatly impacted by the addition of heterocyclic rings.

Scheme

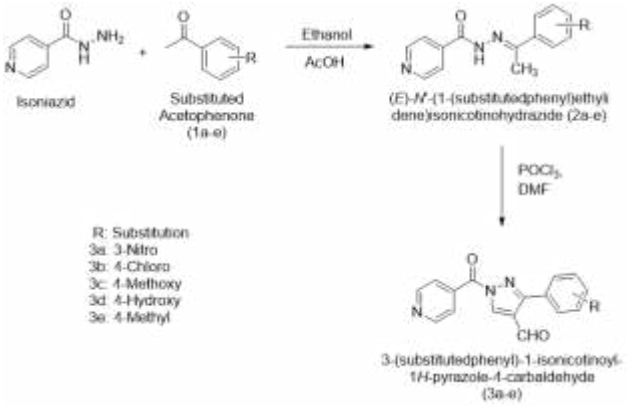

Table: List of Substitution

Compound Code	Substitution (R)
3a	3-Nitro
3b	4-Chloro
3c	4-Methoxy
3d	4-Hydroxy
3e	4-Methyl

Materials

List of Chemicals

S. No.	Chemical Name	Grade	Manufacturer
1	Substituted Acetophenones	AR Grade	Sigma-Aldrich, USA
2	Furan-2-carbaldehyde	AR Grade	Merck Life Science Pvt. Ltd., India
3	Sodium Hydroxide (NaOH)	AR Grade	Loba Chemie Pvt. Ltd., India
4	Sodium Bicarbonate	AR	Merck Life Science Pvt. Ltd., India
5	Hydrochloric Acid	AR	Sisco Research Laboratories (SRL), India
6	Glacial Acetic Acid	AR	Rankem (Avantor), India
7	Ethanol (Absolute)	AR	Changshu Yangyuan Chemicals, China
8	Methanol	AR	Merck Life Science Pvt. Ltd., India
9	Chloroform	AR	Rankem (Avantor), India
10	Ethyl Acetate	AR	Loba Chemie Pvt. Ltd., India
11	n-Hexane	AR	S.D. Fine Chemicals Ltd., India
12	Benzene	AR Grade	Merck Life Science Pvt. Ltd., India
13	Petroleum Ether	AR Grade	Loba Chemie Pvt. Ltd., India
14	Dimethyl Sulfoxide (DMSO)	AR	Sigma-Aldrich, USA
15	Dimethylformamide (DMF)	AR	Merck Life Science Pvt. Ltd., India
16	2-Hydrazinyl Benzothiazole	AR Grade	Sigma-Aldrich, USA
17	2,2-Diphenyl-1-picrylhydrazyl (DPPH)	Analytical Grade	Sigma-Aldrich, USA
18	Ascorbic Acid	Reference Standard	Sigma-Aldrich, USA
19	Potassium Bromide (KBr)	Spectroscopic Grade	Merck Life Science Pvt. Ltd., India
20	Deuterated DMSO (DMSO-d_6)	NMR Grade	Cambridge Isotope Laboratories, USA
21	Silica Gel-G	Chromatographic Grade	Merck Life Science Pvt. Ltd., India
22	Silica Gel GF_{254} (TLC grade)	—	Merck Life Science Pvt. Ltd., India
23	Distilled Water	Laboratory Grade	In-house Laboratory Supply

Methodology

Design of Target Compounds

The design of the target compounds, namely substituted isoniazid–pyrazole hybrid derivatives, was carried out using a rational drug design approach based on the principles of medicinal chemistry, molecular hybridization, and structure–activity relationship (SAR) studies. The primary objective of the molecular design was to develop novel heterocyclic hybrid scaffolds possessing enhanced antibacterial potential through the strategic combination of pharmacologically active moieties within a single molecular framework.

The design strategy involved the integration of the isoniazid nucleus, a well-established antimicrobial pharmacophore, with a substituted pyrazole ring system known for its broad spectrum of biological activities. The resulting hybrid molecules were expected to exhibit improved antibacterial efficacy, enhanced binding interactions with microbial target proteins, and reduced susceptibility toward bacterial resistance mechanisms.

The designed compounds were synthesized through a multistep reaction sequence involving the formation of hydrazone intermediates followed by cyclization reactions to obtain substituted pyrazole derivatives. Different substituted aromatic groups were introduced into the pyrazole framework to modulate electronic distribution, steric properties, lipophilicity, and biological interactions. The selection of substituents was based on their reported influence on antimicrobial activity and their ability to affect ligand–receptor interactions through electronic and hydrophobic effects.

Rationale for Substituted Phenyl Groups

The incorporation of substituted phenyl rings into the pyrazole scaffold was strategically undertaken to investigate the influence of electronic, steric, and hydrophobic factors on antibacterial activity. Aromatic substitutions are well known to significantly alter the pharmacological behavior of heterocyclic compounds by affecting molecular stability, target binding affinity, membrane permeability, and overall physicochemical properties.

In the present study, both electron-donating and electron-withdrawing substituents were introduced on the phenyl ring attached to the pyrazole nucleus to generate structurally diverse analogues. Electron-donating groups such as methoxy, methyl, and hydroxy substituents were expected to increase electron density within the aromatic system, thereby enhancing π–π stacking interactions and hydrogen bonding with amino acid residues present in the active site of bacterial enzymes. These substituents may also improve lipophilicity and facilitate better penetration through bacterial cell membranes.

On the other hand, electron-withdrawing substituents such as nitro and chloro groups were incorporated to enhance electrophilic character and modulate intermolecular interactions with microbial targets. These groups are known to influence molecular polarity and may improve binding affinity through dipole–dipole interactions and electrostatic attraction with active site residues of bacterial proteins.Steric considerations were also taken into account during molecular design. The position and nature of substituents on the phenyl ring can alter the spatial arrangement of the molecules, thereby affecting conformational flexibility and orientation within the binding pocket of bacterial enzymes. Variations in substitution patterns were therefore expected to influence antibacterial potency and selectivity.

Accordingly, a series of substituted phenyl derivatives were designed containing nitro, chloro, methoxy, hydroxy, and methyl groups to systematically evaluate the impact of electronic and steric modifications on biological activity

through antibacterial screening and molecular docking studies.

Hybridization Strategy (Isoniazid–Pyrazole)

In the present investigation, two pharmacologically important moieties, namely isoniazid and pyrazole, were integrated to obtain novel hybrid scaffolds with potential antibacterial activity. The rationale behind this approach was to combine the established antimicrobial properties of isoniazid with the diverse biological activities of pyrazole derivatives to achieve synergistic pharmacological effects.

Synthetic Scheme Mechanism

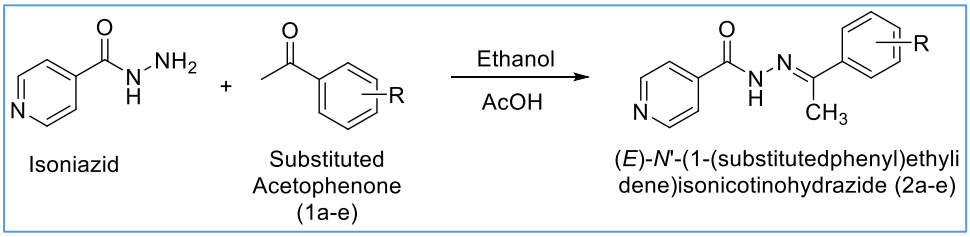

Reaction I: Formation of Acetophenone Hydrazone by condensation of acetophenone with hydrazine

Wolff–Kishner reduction Reaction

The Wolff–Kishner reduction of acetophenone begins with the condensation of acetophenone and hydrazine hydrate (H_2NNH_2) to produce acetophenone hydrazone as the key intermediate. This initial condensation step is one of the most important stages of the Wolff–Kishner reaction pathway and involves nucleophilic addition followed by dehydration.

Acetophenone contains a reactive carbonyl group (>C=O), in which the carbon atom possesses partial positive character due to the electronegativity difference between carbon and oxygen. Hydrazine, containing two amino groups, acts as a strong nucleophile and attacks the electrophilic carbonyl carbon of acetophenone. Under acidic or mildly heated conditions, the lone pair of electrons on the nitrogen atom of hydrazine attacks the carbonyl carbon, resulting in the formation of an unstable tetrahedral intermediate known as a carbinolamine intermediate.

The mechanism of hydrazone formation can be represented as follows:

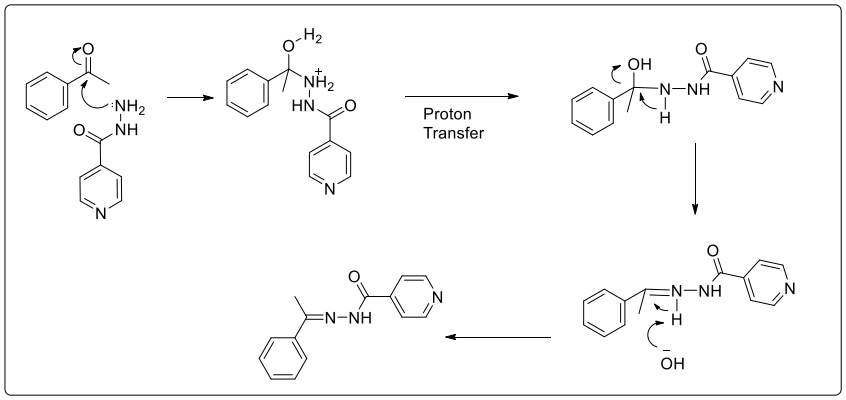

Fig 4.1 ***Wolff–Kishner reduction Reaction Mechanism***

Reaction II: Formation of pyrazole Ring by Reaction of Acetophenone Hydrazone with Vilsmaier Hack Reagent

Vilsmaier Hack Reaction

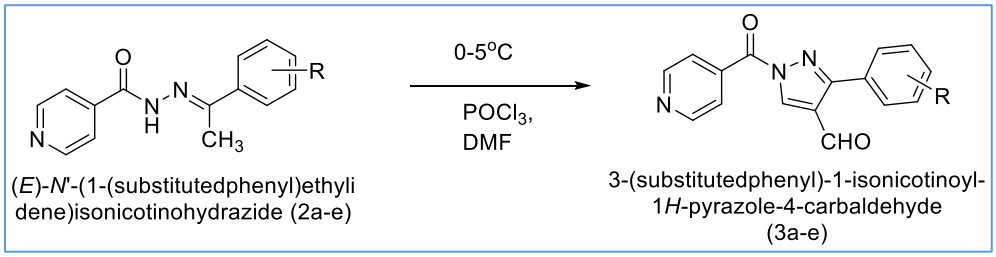

The conversion of acetophenone hydrazone derivatives into substituted pyrazole-4-carbaldehyde derivatives was carried out using the Vilsmeier–Haack reagent generated from phosphorus oxychloride ($POCl_3$) and dimethylformamide (DMF). This reaction represents an important synthetic transformation in heterocyclic chemistry and is widely employed for cyclization and formylation reactions leading to nitrogen-containing heterocyclic systems.

In the present study, the Vilsmeier–Haack reaction played a dual role by facilitating both cyclization of the hydrazone intermediate and introduction of a formyl group at the 4-position of the pyrazole ring. The reaction proceeds through the formation of an electrophilic iminium ion species, commonly known as the Vilsmeier reagent, which subsequently reacts with the hydrazone substrate to generate the pyrazole scaffold.

The detailed reaction mechanism is discussed below:

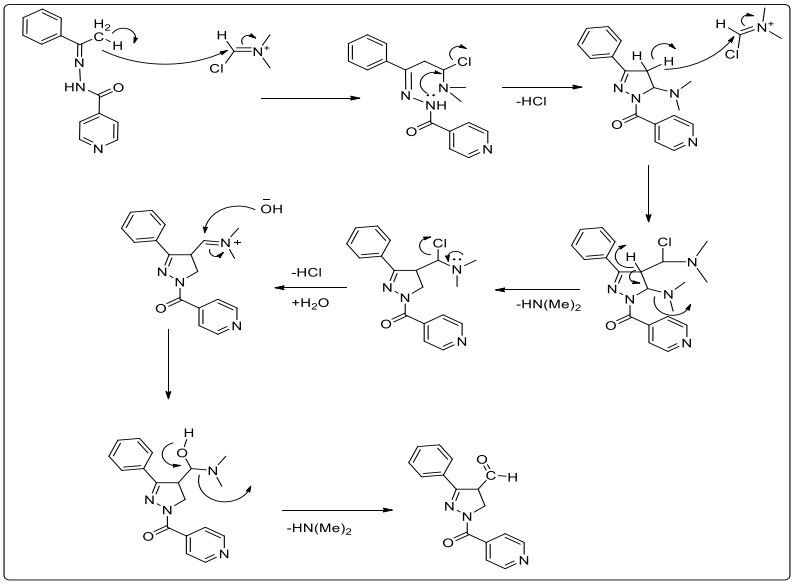

Fig.: ***Vilsmaier Hack Reaction Mechanism***

Synthetic Procedure of Designed Compounds

Synthesis of (E)-N'-(1-(Substituted-Phenyl)ethylidene) Isonicotinohydrazide Derivatives (2a–e)

A series of substituted hydrazone derivatives, namely (E)-N′-(1-(substituted phenyl)ethylidene)isonicotinohydrazides (2a–e), were synthesized through a condensation reaction between isoniazid and various substituted acetophenones. isoniazid (0.014 mol) and the respective substituted acetophenone derivative (0.015 mol) were transferred into a 50 mL RBF containing 20 mL of absolute ethanol as the reaction solvent.

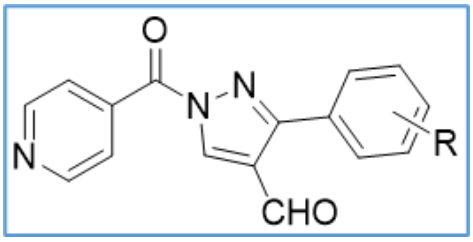

The reaction mixture was stirred continuously and initially maintained at low temperature (approximately 0 °C) using an ice bath. Subsequently, 3-4 drops of acetic acid were carefully introduced as an acid catalyst to promote hydrazone formation. After complete mixing of the reactants, the temp of the reaction system was gradually increased, and the mixture was subjected to reflux at approximately 60 °C for 2–3 hours, reaction was monitored at regular intervals by TLC using a suitable solvent system. Upon completion of the reaction, the hot reaction mixture was slowly poured into crushed ice with constant stirring, leading to the precipitation of the desired hydrazone intermediate.

The resulting solid product was separated by vacuum filtration and washed repeatedly with cold distilled water to remove traces of unreacted materials and acidic impurities. The purified precipitate was then dried at room temperature or in a desiccator until a constant weight was obtained.

Synthesis of 3-(substitutedphenyl)-1-isonicotinoyl-1H-pyrazole-4-carbaldehyde (3a-e)

Dimethylformamide (DMF, 40 mmol) was transferred into a clean, dry round-bottom flask equipped with a magnetic stirrer and maintained under cooling conditions using an ice bath to control the exothermic nature of the reaction. The previously synthesized hydrazone intermediate, (E)-N′-(1-(substituted phenyl)ethylidene)isonicotinohydrazide (12 mmol), was then added gradually to the chilled DMF solution under continuous stirring to obtain a homogeneous reaction mixture. Subsequently, $POCl_3$, 40 mmolwas added dropwise with constant stirring while maintaining the temperature below 5 °C during the addition process. The slow addition of $POCl_3$ was essential to prevent excessive heat generation and to ensure controlled formation of the Vilsmeier–Haack electrophilic reagent. During this stage, the interaction between DMF and $POCl_3$ generated the reactive chloromethyleneiminium ion, which facilitated cyclization and formylation of the hydrazone substrate.

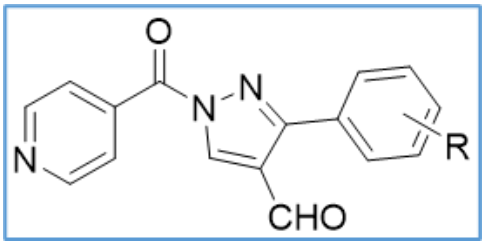

After complete addition of $POCl_3$, the cooling bath was removed and the reaction mixture was gradually heated to approximately 60 °C. The reaction was maintained at this temperature under continuous stirring for nearly 6 hours.

Upon completion, the hot reaction mixture was carefully poured onto crushed ice with vigorous stirring. This step resulted in decomposition of the reaction complex and facilitated precipitation of the crude pyrazole derivative. The acidic reaction medium was subsequently neutralized by slow addition of saturated potassium carbonate solution until the evolution of carbon dioxide ceased and the pH became nearly neutral. Neutralization aided in complete precipitation of the product and removal of excess acidic reagents.

The separated solid product was collected by vacuum filtration and washed several times with chilled distilled water. The obtained crude product was then dried under ambient conditions or in a desiccator.Further purification of the synthesized compounds was achieved by recrystallization using ethanol as the solvent system.

Purification of Synthesized Compounds

Recrystallization

The crude products obtained after completion of the synthetic reactions were purified by recrystallization to obtain compounds of high purity and definite crystalline nature. Ethanol was selected as the recrystallization solvent because of its suitable dissolving capacity for the synthesized derivatives at elevated temperature and poor solubility at lower temperatures.

Initially, the crude compound was transferred into a clean conical flask and dissolved in the minimum possible quantity of hot ethanol with continuous heating. The hot solution was filtered when necessary to remove insoluble impurities. The clear filtrate was then allowed to cool gradually at room temperature to facilitate slow crystal formation. For complete crystallization, the solution was further cooled in an ice bath for a specific period of time.The separated crystals were collected by filtration under reduced pressure and washed carefully with small portions of chilled ethanol to remove traces of adhering impurities and colored materials. The purified crystals were dried at room temperature or in a vacuum desiccator until constant weight was achieved. Recrystallization was repeated whenever required to obtain analytically pure compounds suitable for characterization and biological evaluation.

TLC Analysis

TLC was employed as a simple, rapid, and effective analytical technique for monitoring the progress of the reactions and evaluating the purity of the synthesized compounds. Precoated silica gel-G plates were utilized as the stationary phase, while a solvent system comprising toluene and ethyl acetate in 7:3 was used as the mobile phase for chromatographic separation.

Percentage Yield and Physical Characterization

Percentage Yield

The percentage yield of each synthesized compound was calculated in order to determine the efficiency and reproducibility of the synthetic method employed. The yield was estimated after purification and drying of the final products using the following equation:

$$\%\ Yield = \frac{Practical\ Yield}{Theoretical\ Yield} \times 100$$

Physical Properties

The synthesized compounds were evaluated for various physical characteristics such as appearance, color, crystalline nature, solubility behavior, and melting point. Most of the synthesized derivatives were obtained as crystalline solids exhibiting shades ranging from light yellow to dark yellow or pale brown depending upon the nature of substituent groups present on the aromatic ring.

Characterization of Synthesized Compounds

FT-IR Spectroscopy

Fourier Transform Infrared spectroscopy was employed for identification of important functional groups and confirmation of structural modifications occurring during synthesis. The IR spectra of the synthesized compounds were recorded using an FT-IR spectrophotometer within the spectral region of 4000–400 cm^{-1}. Samples prepared in the form of potassium bromide (KBr) pellets or as thin films depending on the physical properties of the compounds.

The recorded spectra were analyzed for bands corresponding to such as carbonyl (C=O), azomethine (C=N), aromatic C=C stretching, aldehydic C–H, N–N stretching, and heterocyclic vibrations associated with the pyrazole ring. Particular emphasis was placed on disappearance and appearance of specific absorption peaks that confirmed conversion of hydrazone intermediates into the desired pyrazole derivatives.

H NMR Spectroscopy

NMR was carried out for detailed structural elucidation and confirmation of the synthesized compounds. The spectra were recorded using a high-resolution NMR spectrometer operating at an appropriate frequency, generally around 400 MHz. The samples were dissolved in deuterated solvents such as dimethyl sulfoxide-d_6 (DMSO-d_6) or deuterated chloroform ($CDCl_3$), depending on their solubility characteristics. TMS was used as the internal reference standard.

The obtained spectra were interpreted by analyzing chemical shift values (δ ppm), signal multiplicity, coupling constants, and integration patterns. These spectral parameters provided valuable information regarding the number, type, and chemical environment of hydrogen atoms present within the synthesized molecules. Characteristic proton signals corresponding to aromatic protons, aldehydic proton, pyrazole ring protons, and amide functionalities were carefully examined to confirm the proposed molecular structures.

Mass Spectrometry

Mass spectrometric analysis was performed to determine the molecular masses and to further support the structural identity of the synthesized compounds. Depending upon the nature and stability of the samples, suitable ionization techniques such as Electrospray Ionization Mass Spectrometry (ESI-MS) or Gas Chromatography–Mass Spectrometry (GC-MS) were employed.

The mass spectra were carefully analyzed for the presence of molecular ion peaks corresponding to the expected molecular weights of the synthesized derivatives. The protonated molecular ion peaks generally appeared in the form of $[M+H]^+$ ions, which confirmed the molecular mass of the compounds.

In addition to molecular ion peaks, fragmentation patterns observed in the spectra provided important structural information regarding cleavage pathways and stability of different fragments. The experimentally observed mass values were compared with theoretically calculated molecular weights, and close agreement between the two further confirmed successful synthesis and purity of the target compounds.

Molecular Docking Study

Molecular docking studies were carried out to investigate the binding affinity, interaction pattern, and possible inhibitory potential of the synthesized isoniazid–pyrazole hybrid scaffolds against selected bacterial target proteins. Docking analysis provides valuable information regarding ligand–receptor interactions at the molecular level and plays an important role in rational drug design by predicting the preferred orientation of a ligand within the active.

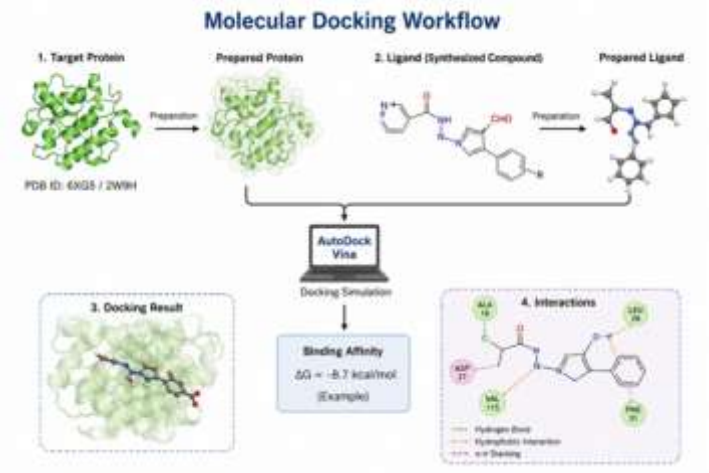

Fig. Molecular Docking Workflow

The synthesized compounds were docked against two bacterial enzymes associated with microbial growth and survival, namely Escherichia coli dihydrofolate reductase (DHFR) and Staphylococcus aureus dihydrofolate reductase (DHFR). Dihydrofolate reductase is an essential enzyme involved in folate metabolism and nucleic acid biosynthesis, making it an important target for antibacterial drug development. Inhibition of DHFR disrupts the synthesis of tetrahydrofolate, thereby interfering with bacterial DNA replication and cell proliferation.

3D crystal structures of the target proteins were obtained from the PDB. The selected proteins included:

- **Escherichia coli dihydrofolate reductase (DHFR) – PDB ID: 6XG5**
- **Dihydrofolate reductase (DHFR) – PDB ID: 2W9H**

The molecular docking experiments were performed using **AutoDock Vina(MGL Tools version 1.5.7)**. The software was selected because of its reliability, computational efficiency, and wide application in structure-based drug discovery studies.

Evaluation of Antibacterial Activity

The synthesized isoniazid–pyrazole hybrid derivatives (3a–e) were evaluated for their antibacterial activity by employing an in vitro agar disk diffusion method against selected bacterial isolates. The study was performed to investigate the inhibitory potential of the synthesized compounds and to compare their antibacterial efficacy with that of the standard drug isoniazid.

Measurement of Antibacterial Activity

After completion of incubation, the antibacterial activity was assessed by measuring the diameter of the clear zones of inhibition formed around each disk. The zones of inhibition were measured in millimeters using a calibrated scale or zone reader.Compounds exhibiting larger inhibition zones were considered to possess greater antibacterial activity.

RESULT & DISCUSSION

Molecular Docking Study of Synthesized Compounds

Molecular Docking Study Against Staphylococcus aureus Dihydrofolate Reductase (DHFR) (PDB ID: 2W9H)

The synthesized isoniazid–pyrazole hybrid derivatives (3a–3e) were subjected to molecular docking studies against Staphylococcus aureus Dihydrofolate Reductase (DHFR) usingAutoDock Vina in order to evaluate their binding affinity and interaction pattern within the active site of the target protein. Trimethoprim, a well-known DHFR inhibitor, was used as the reference standard for comparative analysis.

Table 5.1Molecular DockingInteraction and binding affinity ofStaphylococcus aureus Dihydrofolate Reductase (DHFR) (PDB ID: 2W9H)

Comp	Binding Energy (kcal/mol)	Binding Interactions	
		H-Bonding	Pi-alkyl/ Alkyl
3a	**-9.3**	Thr46	Lys45 & Leu 20
3b	**-8.7**	Ser49	Lys45, Val6, & Ile14
3c	-9.4	Thr96	Lys45, Phe98 & Val6
3d	**-8.4**	-	Lys45
3e	-9.0	Ser49	Lys45, Ile14, Val6 & Phe98
Std. (Trimethoprim)	-7.2	Asp27, Ala7 & Ile14	Leu20

The docking scores of the synthesised compounds varied from –8.4 to –9.4 kcal/mol, whereas trimethoprim exhibited a lower binding energy of –7.2 kcal/mol, indicating a comparably weaker ligand–protein interaction. Among the synthesised derivatives, molecule 3c demonstrated the greatest binding affinity, with a docking score of –9.4 kcal/mol. The molecule established hydrogen bonding with Thr96 and hydrophobic contacts with Lys45, Phe98, and Val6 residues, perhaps enhancing the ligand's stability inside the active binding pocket. Compound 3a exhibited remarkable binding affinity, shown by a docking score of –9.3 kcal/mol, and formed hydrogen bonds with Thr46, in addition to π-alkyl interactions with Lys45 and Leu20. Compound 3e exhibited a robust contact with the target protein, achieving a docking score of –9.0 kcal/mol, accompanied by hydrogen bonding with Ser49 and supplementary hydrophobic interactions with Lys45, Ile14, Val6, and Phe98 residues.

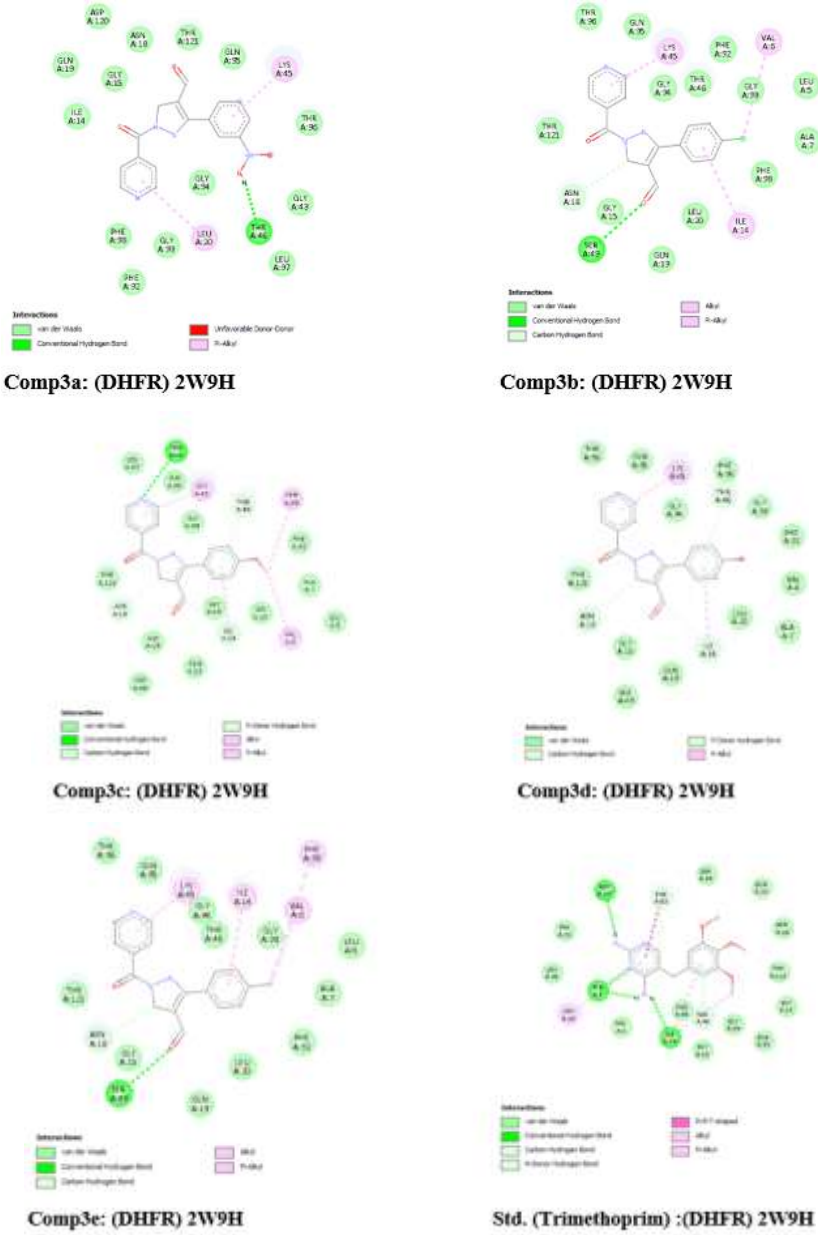

Fig. 2D Interaction of Synthesized compounds (3a-ae) with Staphylococcus aureus Dihydrofolate Reductase (DHFR) (PDB ID: 2W9H)

Compound 3b had strong binding affinity with a docking score of –8.7 kcal/mol, establishing hydrogen bond interactions with Ser49 and alkyl contacts with Lys45, Val6, and Ile14. These interactions indicated a favourable orientation and stable positioning of the ligand inside the enzyme's active region. Conversely, compound 3d exhibited the lowest binding affinity among the synthesised derivatives, with a docking score of –8.4 kcal/mol. The somewhat diminished docking score of this molecule may be ascribed to the lack of hydrogen bonding contacts, since only alkyl interaction with Lys45 was noted. The reduced number of stabilising contacts likely resulted in a lower binding affinity compared to the other synthesised compounds.

Molecular Docking Study Against synthesized compounds with Escherichia coli dihydrofolate reductase (DHFR) – PDB ID: 6XG5

The molecular docking investigation of the synthesised isoniazid–pyrazole hybrid compounds (3a–3e) against the DHFR enzyme (PDB ID: 2W9H) demonstrated advantageous binding interactions and substantial binding affinity for the active site of the target protein. The docking scores of the synthesised compounds varied from –8.5 to –8.9 kcal/mol, whereas the conventional medication trimethoprim had a lower binding energy of –7.7 kcal/mol. The reduced docking energy values for the synthesised variants suggest enhanced ligand–protein interactions and increased stability of the docked complexes relative to the reference medication.

Table: Molecular Docking Interaction and binding affinity of synthesized compounds with Escherichia coli dihydrofolate reductase (DHFR) – PDB ID: 6XG5

Comp	Binding Energy (kcal/mol)	Binding Interactions	
		H-Bonding	Pi-alkyl/ Alkyl/ pi-pi Stacked
3a	**-8.5**	Thr46 & Ser49	Ala7, Met20 & Phe31
3b	**-8.9**	Met20	Ala7, Ile14, Ile5 & Phe31
3c	-8.7	Thr46 & thr123	Ile14, Arg98 & His45
3d	**-8.7**	Met20	Ala7, Ile14, Ile5 & Phe31
3e	-8.7	Met20	Ile14, Ala7, Phe31 & Trp30
Std. (Trimethoprim)	-7.7	Thr113, Ile94, Ile5, Tyr100	Phe81

Among the synthesized compounds, derivative 3b demonstrated the highest binding affinity with a docking score of –8.9 kcal/mol. The compound formed hydrogen bonding interaction with Met20 and additional hydrophobic interactions involving Ala7, Ile14, Ile5, and Phe31 residues, which contributed toward stable binding within the active site cavity. Compound 3c also exhibited strong binding affinity with a docking score of –8.7 kcal/mol and formed hydrogen bond interactions with Thr46 and Thr123 along with hydrophobic interactions involving Ile14, Arg98, and His45 residues.

Similarly, compounds 3d and 3e displayed docking scores of –8.7 kcal/mol. Compound 3d showed hydrogen bonding with Met20 and alkyl interactions involving Ala7, Ile14, Ile5, and Phe31, whereas compound 3e formed hydrogen bond interaction with Met20 along with hydrophobic interactions involving Ile14, Ala7, Phe31, and Trp30 residues. Compound 3a exhibited a docking score of –8.5 kcal/mol and interacted with the target enzyme through hydrogen bonding with Thr46 and Ser49 along with π-alkyl interactions involving Ala7, Met20, and Phe31.

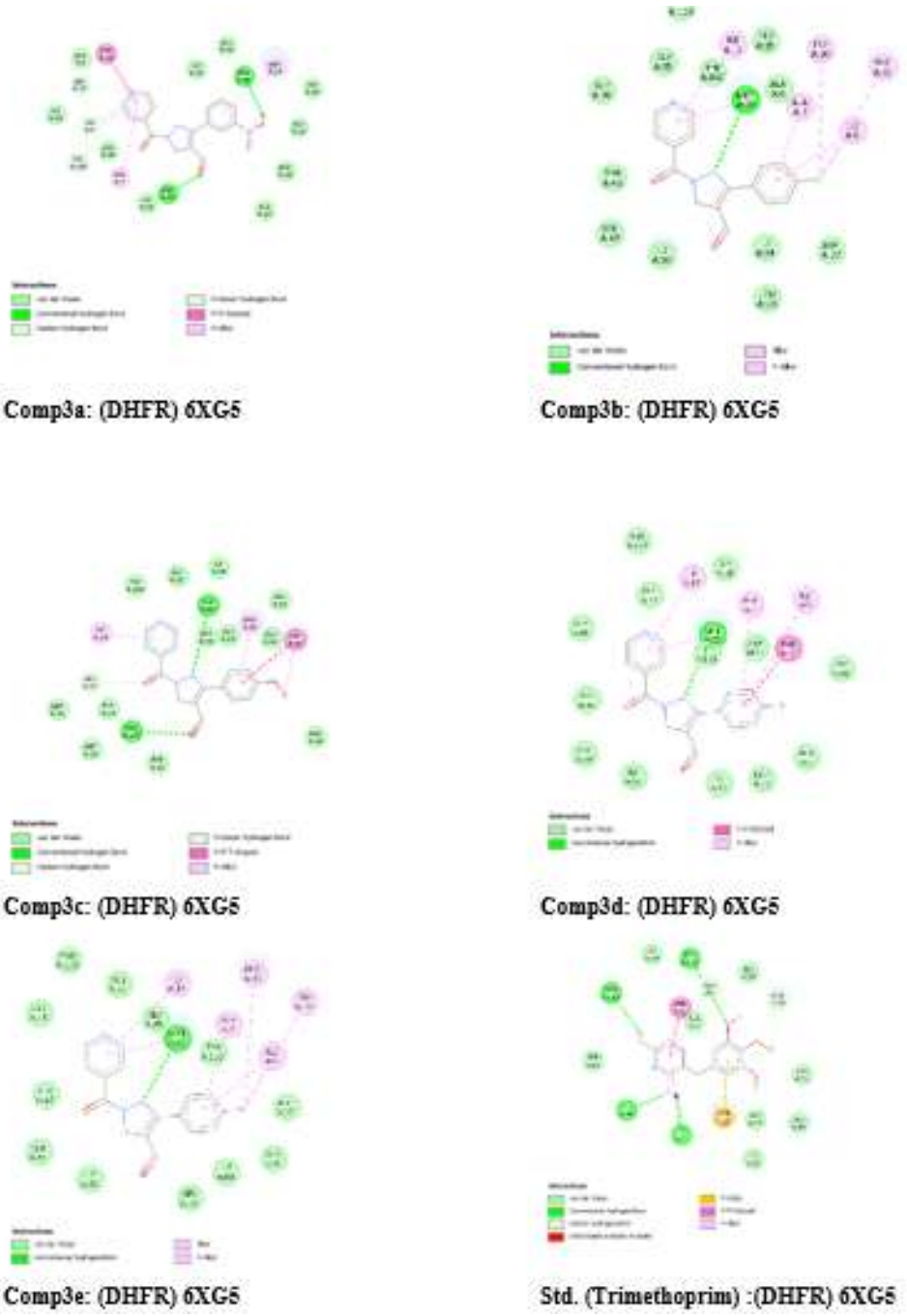

Fig. 2D Interaction of Synthesized compounds (3a-ae) withEscherichia coli dihydrofolate reductase (DHFR) – PDB ID: 6XG5

Result of Synthesis

(E)-N′-(1-(SubstitutedPhenyl)ethylidene)Isonicotinohydrazide Derivatives (2a–e)

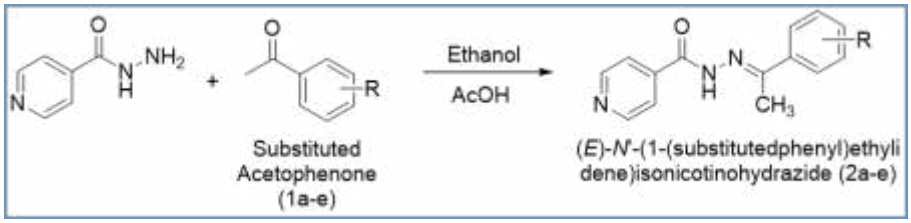

Table: Physiochemical Properties of synthesized derivatives (2a-e)

Comp.	Substituent (R)	Appearance	Mol. Wght (g/mol)	Yield (%)	M.P. (°C)	Rf Value
2a	3-NO_2	Yellow crystalline solid	284.27	78.5	198–201	0.62
2b	4-Cl	Pale yellow crystalline solid	273.72	81.3	186–189	0.66
2c	4-OCH_3	Light yellow crystalline solid	269.31	84.6	174–177	0.58
2d	4-OH	Creamish yellow crystalline solid	255.28	76.9	210–213	0.49
2e	4-CH_3	Yellow crystalline solid	253.31	82.1	168–171	0.71

TLC solvent: Toluene: Ethyl Acetate (7:3)

3-(substitutedphenyl)-1-isonicotinoyl-1Hpyrazole-4carbaldehyde (3a-e)

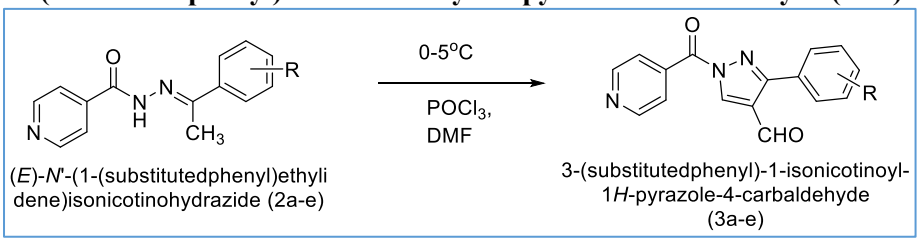

1-isonicotinoyl-3-(3-nitrophenyl)-1H-pyrazole-4-carbaldehyde (3a)

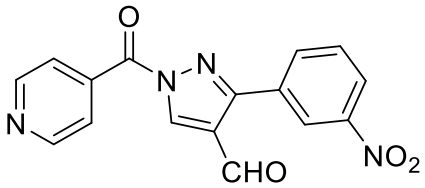

Parameter	Observation
Mol Wght	322.28
Mol For	$C_{16}H_{10}N_4O_4$
Substituent (R)	3-NO_2
Appearance/Color	Pale yellow
Nature	Crystalline solid
Yield (%)	72
Melting Point (°C)	287-289
Rf Value	0.63
Solubility	Soluble in DMSO, methanol; slightly soluble in ethanol; insoluble in water

FT-IR Spectra (Kbr):

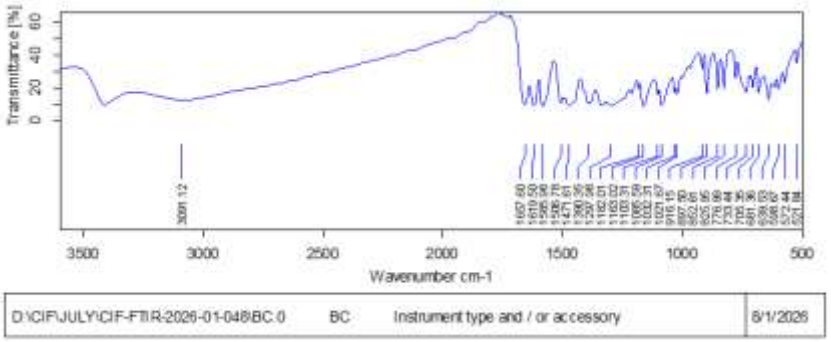

Functional Group	Expected Range (cm^{-1})	Observed Value (cm^{-1})
Ar C–H stretching	3000–3100	3091.12
N–C=O (Amide carbonyl)	1640–1690	1657.82
Ar C=C stretching	1450–1600	1601.50, 1568.69
Pyridine C–N stretching	1320–1380	1327.98
C–N stretching (Pyrazole)	1200–1300	1242.80
N–N stretching (Pyrazole)	1010–1090	1022.31
NO_2 symmetric stretching	1340–1380	1363.07

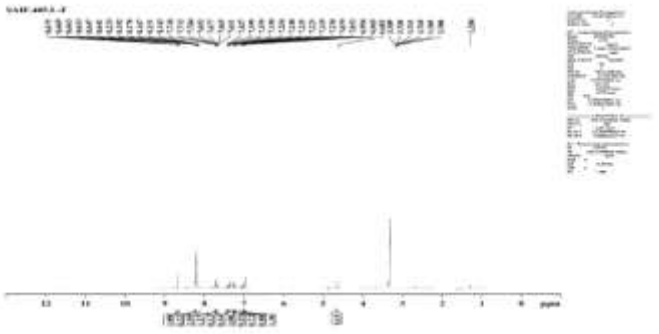

NMR Spectra	Observed δ (ppm)
Aromatic protons (Ar–H)	6.994-8.669 (m, 9 H, Ar-H)
C-H (aldehyde)	4.675 (s, 1H, CH=O)

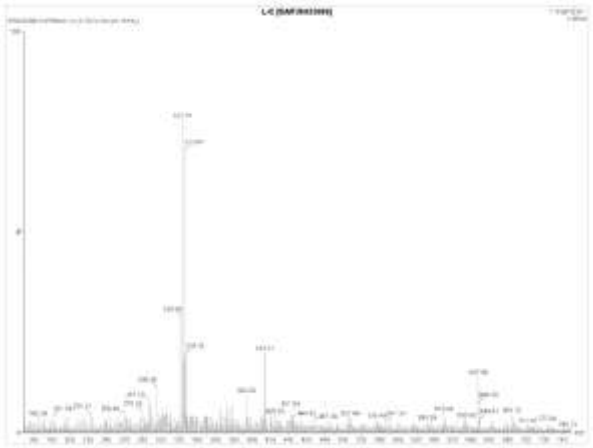

Parameter	Observation
Mol Wght	311.73
Mol For	$C_{16}H_{10}ClN_3O_2$
Substituent (R)	4-Cl
Appearance/Color	Yellow
Nature	Crystalline solid
Yield (%)	76
Melting Point (°C)	271-273
Rf Value	0.54
Solubility	Soluble in DMSO, methanol; slightly soluble in ethanol; insoluble in water

Mass Spectra: 322.53 [M+], 323.61 [M+1]

3-(4Chlorophenyl)-1-isonicotinoyl-1Hpyrazole-4carbaldehyde (3b)

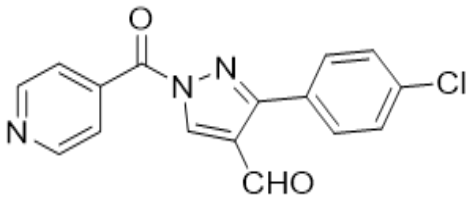

FT-IR Spectra (Kbr):

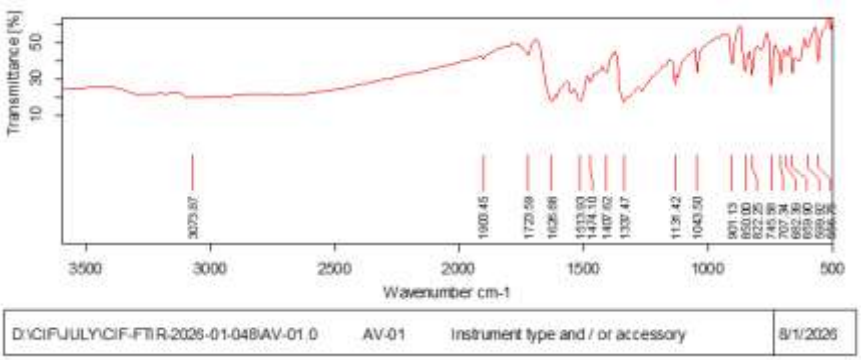

Functional Group	Expected Range (cm^{-1})	Observed Value (cm^{-1})
Ar C–H stretching	3000–3100	3058.42
N–C=O (Amide carbonyl)	1640–1690	1662.31
Ar C=C stretching	1450–1600	1598.74
Pyridine C–N stretching	1320–1380	1334.27
C–N stretching (Pyrazole)	1200–1300	1248.53
N–N stretching (Pyrazole)	1010–1090	1036.18
C–Cl stretching	700–850	782.46

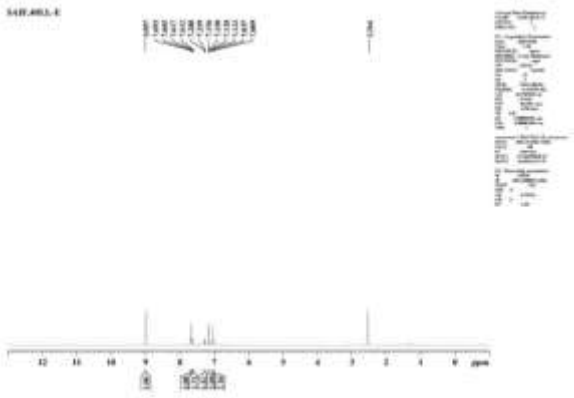

NMR Spectra	Observed δ (ppm)
Aromatic protons (Ar–H)	7.009-7.693 (m, 9 H, Ar-H)
C-H (aldehyde)	9.057 (s, 1H, CH=O)

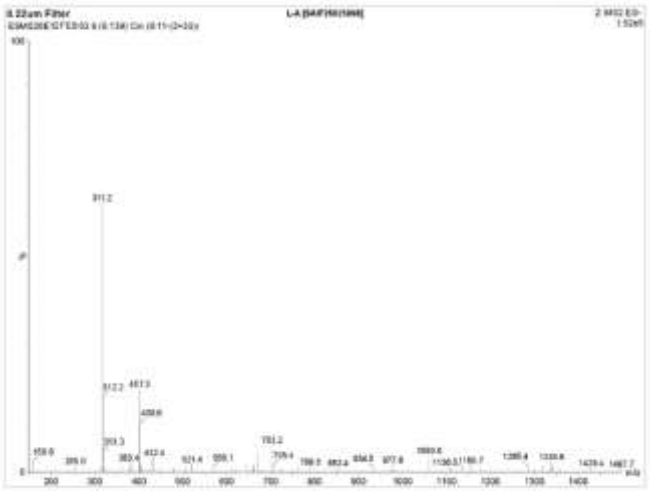

Mass Spectra: 311 [M+], 313 [M+2]

1-isonicotinoyl-3-(4methoxyphenyl)-1Hpyrazole-4carbaldehyde (3c)

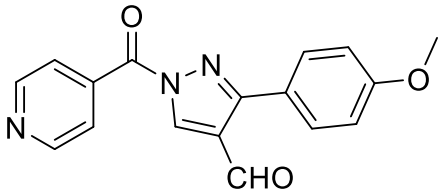

Parameter	Observation
Mol Wght	307.31
Mol For	$C_{17}H_{13}N_3O3$
Substituent (R)	4-OCH_3
Appearance/Color	Pale Brown
Nature	Crystalline solid
Yield (%)	64
Melting Point (°C)	293-295
Rf Value	0.57
Solubility	Soluble in DMSO, methanol; slightly soluble in ethanol; insoluble in water

FT-IR Spectra (KBr**):**

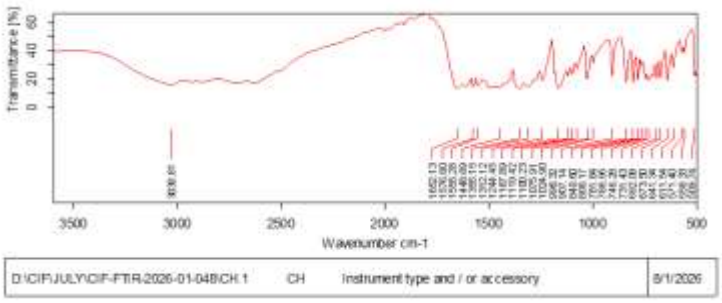

Functional Group	Expected Range (cm^{-1})	Observed Value (cm^{-1})
Ar C–H stretching	3000–3100	3030.81
N–C=O (Amide carbonyl)	1640–1690	1652.13
Ar C=C stretching	1450–1600	1570.88, 1488.78
Pyridine C–N stretching	1320–1380	1365.25
C–N stretching (Pyrazole)	1200–1300	1244.45
N–N stretching (Pyrazole)	1010–1090	1070.93
C–OCH_3 stretching	1020–1275	1244.45, 1170.23

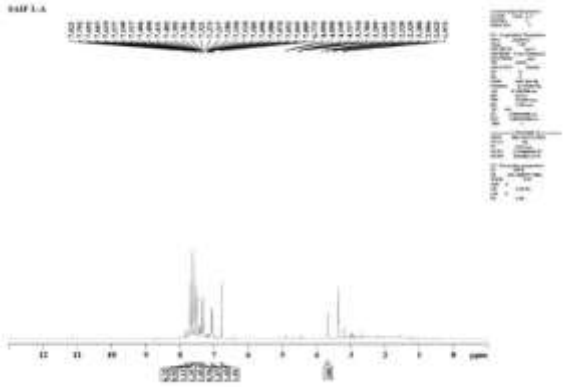

NMR Spectra	Observed δ (ppm)
C-OCH_3	3.299 (s, 3H, CH3)
Aromatic protons (Ar–H)	6.775-7.692 (m, 9 H, Ar-H)
C-H (aldehyde)	7.792 (s, 1H, CH=O)

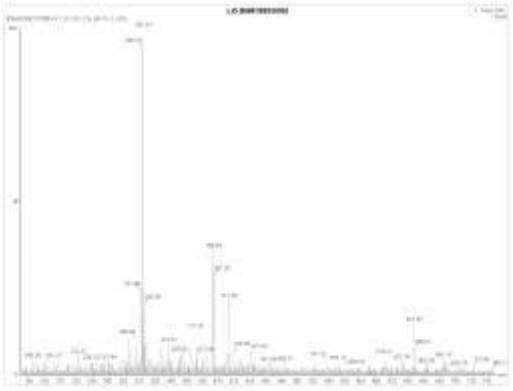

Mass Spectra: 307 [M+], 308 [M+1]

3-(4hydroxyphenyl)-1-isonicotinoyl-1Hpyrazole-4carbaldehyde (3d)

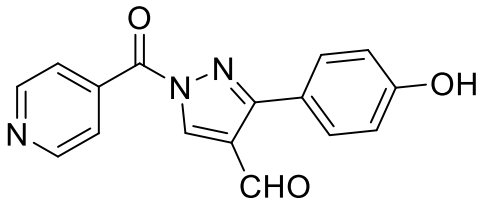

Parameter	Observation
Mol Wght	293.08
Mol For	$C_{16}H_{11}N_3O_3$
Substituent (R)	4-OH
Appearance/Color	Light Brown
Nature	Crystalline solid
Yield (%)	73
Melting Point (°C)	304-306
Rf Value	0.59
Solubility	Soluble in DMSO, methanol; slightly soluble in ethanol; insoluble in water

FT-IR Spectra (Kbr):

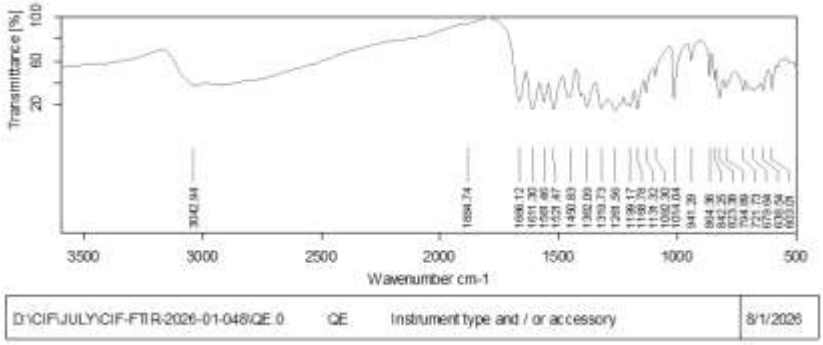

Functional Group	Expected Range (cm^{-1})	Observed Value (cm^{-1})
Ar C–H stretching	3000–3100	3042.94
N–C=O (Amide carbonyl)	1640–1690	1668.12
Ar C=C stretching	1450–1600	1561.46, 1519.49
Pyridine C–N stretching	1320–1380	1328.09
C–N stretching (Pyrazole)	1200–1300	1261.56
N–N stretching (Pyrazole)	1010–1090	1039.04
C–OH stretching	1180–1360	1261.56, 1173.20

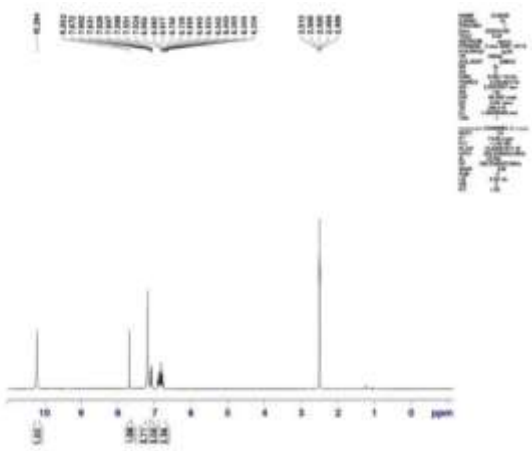

NMR Spectra	Observed δ (ppm)
C-OH	10.264 (s, 1H, OH)
Aromatic protons (Ar–H)	6.625-6.672 (m, 9 H, Ar-H)
C-H (aldehyde)	8.552 (s, 1H, CH=O)

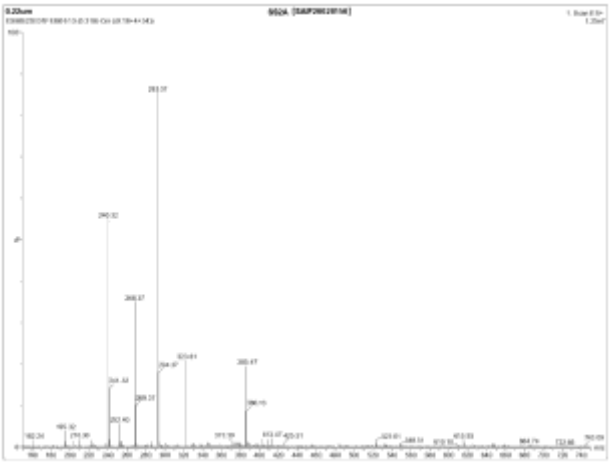

Parameter	Observation
Mol Wght	291.10
Mol For	$C_{17}H_{13}N_3O_2$
Substituent (R)	4-CH_3
Appearance/Color	Brown
Nature	Crystalline solid
Yield (%)	65
Melting Point (°C)	311-313
Rf Value	0.72
Solubility	Soluble in DMSO, methanol; slightly soluble in ethanol; insoluble in water

Mass Spectra: 293.37 [M+], 294.37 [M+1]

1-isonicotinoyl-3-(ptolyl)-1Hpyrazole-4carbaldehyde (3e)

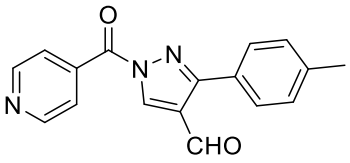

FT-IR Spectra (Kbr):

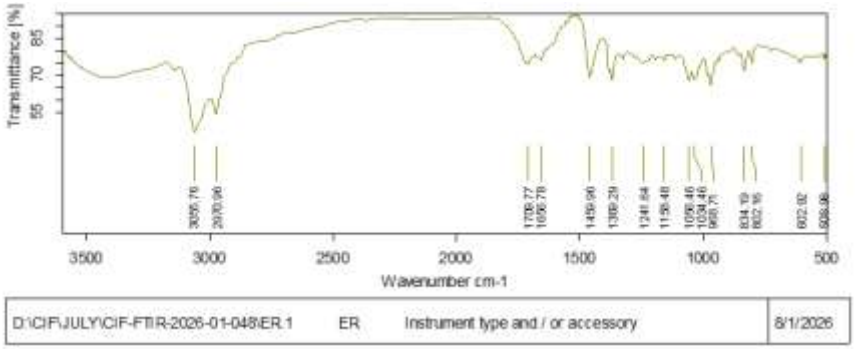

Functional Group	Expected Range (cm^{-1})	Observed Value (cm^{-1})
Ar C–H stretching	3000–3100	3057.76
N–C=O (Amide carbonyl)	1640–1690	1670.77
Ar C=C stretching	1450–1600	1498.84, 1448.29
Pyridine C–N stretching	1320–1380	1369.29
C–N stretching (Pyrazole)	1200–1300	1241.64
N–N stretching (Pyrazole)	1010–1090	1034.46
C–CH_3 stretching	2850–2960	2880.96

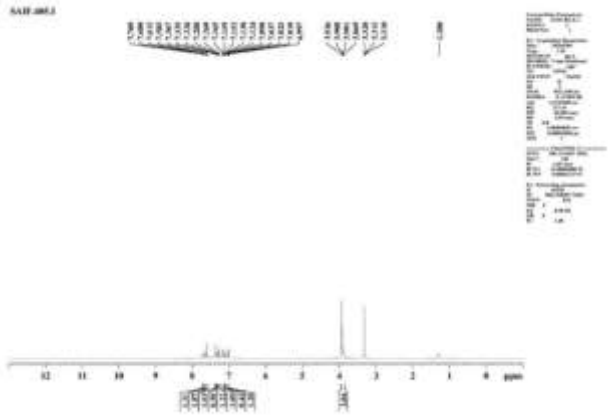

NMR Spectra	Observed δ (ppm)
Ali C-H	3.908 (s, 3H, CH3)
Aromatic protons (Ar–H)	6.997-7.680 (m, 9 H, Ar-H)
C-H (aldehyde)	7.709 (s, 1H, CH=O)

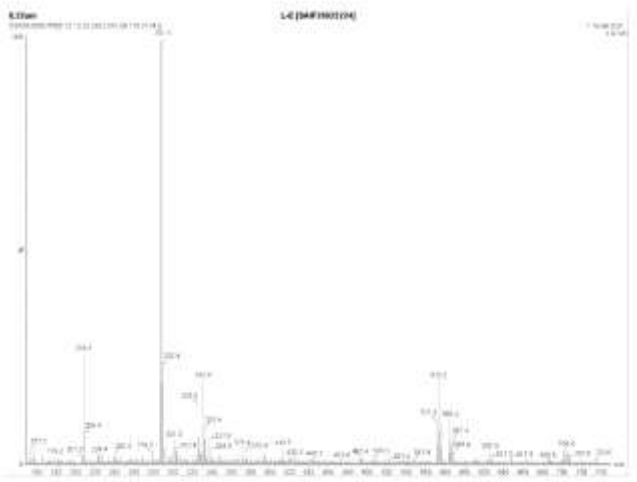

Mass Spectra: 391.3 [M+], 292.4 [M+2]

Antibacterial Activity

The synthesised isoniazid–pyrazole hybrid compounds (3a–3e) were evaluated for their in vitro antibacterial efficacy against specific bacterial strains using the agar disc diffusion technique. The antibacterial effectiveness of the synthesised compounds was assessed by measuring the width of the inhibition zones formed around the impregnated discs after incubation at 37 °C for 24 hours. Isoniazid functioned as the usual antibacterial agent, whilst DMSO acted as the negative control.

Table : Antibacterial Activity of Synthesized Isoniazid–Pyrazole Hybrid Derivatives

Compound	Zone of Inhibition (mm)
3a	19.4 ± 0.42
3b	17.8 ± 0.36
3c	21.6 ± 0.51
3d	16.9 ± 0.28
3e	20.2 ± 0.47
Isoniazid (Std.)	22.8 ± 0.39
DMSO (Control)	Nil

The antibacterial screening findings indicated that all synthesised isoniazid–pyrazole hybrid compounds had significant antibacterial activity against the evaluated bacterial strains. The observed zones of inhibition ranged from 16.9 ± 0.28 mm to 21.6 ± 0.51 mm, indicating significant inhibitory effects of the synthesized compounds on bacterial growth. No antibacterial activity was observed in the DMSO control group, confirming that the solvent did not interfere with the experimental observations. Among the synthesized derivatives, compound 3c exhibited the highest antibacterial activity with a zone of inhibition of 21.6 ± 0.51 mm, which was found to be very close to the activity of the standard drug isoniazid (22.8 ± 0.39 mm). The enhanced antibacterial potential of compound 3c may be attributed to the presence of the methoxy substituent, which possibly improved electronic distribution and lipophilic interactions with bacterial target proteins, thereby facilitating better penetration through the bacterial cell membrane.

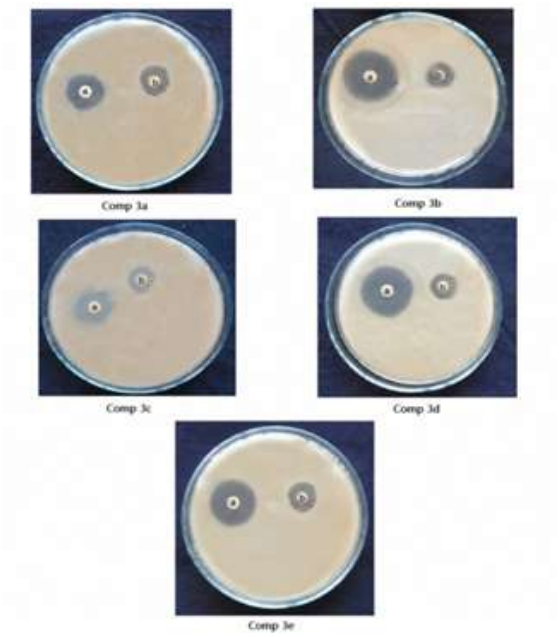

Fig. Antibacterial Activity of Synthesized Isoniazid–Pyrazole

Compound 3e exhibited notable antibacterial activity with an inhibition zone of 20.2 ± 0.47 mm, while compound 3a had significant activity with an inhibition zone of 19.4 ± 0.42 mm. The improved activity of compound 3e may be associated with the hydrophobic nature of the methyl substituent, which possibly enhanced interaction with bacterial cell components. Similarly, the nitro substituent present in compound 3a may have contributed toward enhanced antibacterial action through electron-withdrawing effects and stronger interaction with bacterial enzymes. Compound 3b exhibited moderate antibacterial activity with a zone of inhibition of 17.8 ± 0.36 mm, whereas compound 3d displayed the lowest activity among the synthesized derivatives with a zone of inhibition of 16.9 ± 0.28 mm. The comparatively lower activity of compound 3d may be due to the presence of the hydroxy substituent, which possibly reduced hydrophobic interactions and affected membrane permeability.

Fig. Graph Represents Zone of Inhibition (mm) of Synthesized scaffolds (3a-e)

CONCLUSION

The findings of this research indicate that isoniazid–pyrazole hybrid scaffolds are excellent candidates for the creation of new antibacterial drugs. The integrated results from synthesis, molecular docking, spectroscopic characterisation, and biological assessment suggest that these derivatives have significant promise for future refinement and pharmacological exploration as efficacious antibacterial agents.

REFERENCES

1. World Health Organization. (2023). World Health Statistics 2023: Monitoring Health for the SDGs. World Health Organization, Geneva.
2. World Health Organization. (2020). Global Health Estimates 2019: Deaths by Cause, Age, Sex, by Country and by Region. WHO, Geneva.
3. GBD 2019 Diseases and Injuries Collaborators. (2020). Global burden of 369 diseases and injuries in 204 countries and territories, 1990–2019. The Lancet, 396(10258), 1204–1222.
4. World Health Organization. (2014). Antimicrobial Resistance: Global Report on Surveillance. World Health Organization, Geneva.
5. Murray C.J.L., Ikuta K.S., Sharara F., et al. (2022). Global burden of bacterial antimicrobial resistance in 2019: a systematic analysis. The Lancet, 399(10325), 629–655.
6. Lederberg J., McCray A.T. (2001). 'Ome sweet 'omics—A genealogical treasury of words. The Scientist, 15(7), 8–10.
7. Turnbaugh P.J., Ley R.E., Hamady M., Fraser-Liggett C.M., Knight R., Gordon J.I. (2007). The human microbiome project. Nature, 449, 804–810.
8. World Health Organization. (2021). Climate Change and Health. WHO Fact Sheets. World Health Organization, Geneva.
9. Madigan M.T., Bender K.S., Buckley D.H., Sattley W.M., Stahl D.A. (2021). Brock Biology of Microorganisms. 16th ed. Pearson Education, New York.
10. Tortora G.J., Funke B.R., Case C.L. (2021). Microbiology: An Introduction. 13th ed. Pearson Education, USA.
11. Murray P.R., Rosenthal K.S., Pfaller M.A. (2021). Medical Microbiology. 9th ed. Elsevier, Philadelphia.
12. Willey J.M., Sherwood L.M., Woolverton C.J. (2020). Prescott's Microbiology. 11th ed. McGraw-Hill Education, New York.
13. World Health Organization. (2023). World Health Statistics 2023: Monitoring Health for the SDGs. WHO, Geneva.
14. World Health Organization, *WHO Bacterial Priority Pathogens List, 2024: Bacterial Pathogens of Public Health Importance to Guide Research, Development and Strategies*. Geneva, Switzerland: World Health Organization, 2024.
15. World Health Organization. (2020). Global Tuberculosis Report 2020. WHO, Geneva.
16. R. Laxminarayan *et al.*, "Antimicrobial resistance—The need for global solutions," *The Lancet Infectious Diseases*, vol. 23, no. 7, pp. e219–e229, 2023.
17. Walsh C. (2000). Molecular mechanisms that confer antibacterial drug resistance. Nature. 406:775–781.
18. Blair J.M.A., Webber M.A., Baylay A.J., Ogbolu D.O., Piddock L.J.V. (2015). Molecular mechanisms of antibiotic resistance. Nature Reviews Microbiology. 13:42–51.
19. Davies J., Davies D. (2010). Origins and evolution of antibiotic resistance.

Microbiology and Molecular Biology Reviews. 74(3):417–433.
20. Ventola C.L. (2015). The antibiotic resistance crisis: causes and threats. Pharmacy and Therapeutics. 40(4):277–283.
21. Levy S.B., Marshall B. (2004). Antibacterial resistance worldwide: causes, challenges and responses. Nature Medicine. 10:S122–S129.
22. Thomas C.M., Nielsen K.M. (2005). Mechanisms of, and barriers to, horizontal gene transfer between bacteria. Nature Reviews Microbiology. 3:711–721.
23. Frost L.S., Leplae R., Summers A.O., Toussaint A. (2005). Mobile genetic elements: the agents of open source evolution. Nature Reviews Microbiology. 3:722–732.
24. Donlan R.M., Costerton J.W. (2002). Biofilms: survival mechanisms of clinically relevant microorganisms. Clinical Microbiology Reviews. 15(2):167–193.
25. J. A. Joule and K. Mills, *Heterocyclic Chemistry*, 5th ed. Oxford, U.K.: Wiley-Blackwell, 2010.
26. A. R. Katritzky, C. A. Ramsden, J. A. Joule, and V. V. Zhdankin, *Handbook of Heterocyclic Chemistry*, 3rd ed. Amsterdam, The Netherlands: Elsevier, 2010.
27. T. Eicher, S. Hauptmann, and A. Speicher, *The Chemistry of Heterocycles: Structures, Reactions, Syntheses, and Applications*, 3rd ed. Weinheim, Germany: Wiley-VCH, 2013.
28. C. Walsh, *Antibiotics: Actions, Origins, Resistance*. Washington, DC, USA: ASM Press, 2003.
29. J. Bernstein, W. A. Lott, B. A. Steinberg, and H. L. Yale, “Chemotherapy of experimental tuberculosis. V. Isonicotinic acid hydrazide (INH) and related compounds,” American Review of Tuberculosis, vol. 65, no. 4, pp. 357–364, 1952.
30. A. R. Katritzky, C. W. Rees, and E. F. V. Scriven, *Comprehensive Heterocyclic Chemistry II*, vol. 3. Oxford, U.K.: Pergamon Press, 1996.
31. S. Fustero, M. Sánchez-Roselló, P. Barrio, and A. Simón-Fuentes, “From 1,3-dicarbonyl compounds to pyrazoles: Recent advances in the synthesis and biological applications of pyrazoles,” *Chemical Reviews*, vol. 111, no. 11, pp. 6984–7034, 2011.
32. G. Kumar, S. Yadav, P. Tripathi, A. Verma, S. Singh, and V. Pandey, "Design, synthesis, SAR, and biological investigation of novel isoniazid–rhodanine hybrids as promising anti-tubercular agents," RSC Advances, vol. 15, pp. 31272–31288, 2025.
33. E. Başaran, G. Tür, S. Akkoc and T. Taskin-Tok, “Design, Synthesis, and In Silico and In Vitro Cytotoxic Activities of Novel Isoniazid−Hydrazone Analogues Linked to Fluorinated Sulfonate Esters,” *ACS Omega*, vol. 9, pp. 17551–17562, 2024.
34. Z. M. Elsayed *et al*., “Development of novel isatin–nicotinohydrazide hybrids with potent activity against susceptible/resistant *Mycobacterium tuberculosis* and bronchitis-causing bacteria,” *Journal of Enzyme Inhibition and Medicinal Chemistry*, vol. 36, no. 1, pp. 384–392, 2021.
35. M. D. Johansen *et al.*, "Biological and biochemical evaluation of isatin-isoniazid hybrids as bactericidal candidates against *Mycobacterium tuberculosis*," *Antimicrobial Agents and Chemotherapy*, vol. 65, no. 8, pp. 1-14, 2021.
36. S. R. Shah and K. D. Katariya, “1,3-Oxazole–isoniazid hybrids: Synthesis, antitubercular activity, and their docking studies,” Journal of Heterocyclic Chemistry, vol. 57, no. 2, pp. 1–10, 2020.
37. W. J. Reis, R. A. Santos, B. C. Cavalcanti, M. O. Moraes, R. N. de Oliveira, and R. B. Dias, “Design of hybrid molecules as antimycobacterial compounds: Synthesis of

isoniazid–naphthoquinone derivatives and their activity against susceptible and resistant strains of *Mycobacterium tuberculosis*," *Bioorganic & Medicinal Chemistry*, vol. 27, no. 18, pp. 4143–4150, Sept. 2019.

38. Richard M. Beteck, Ronnett Seldon, Audrey Jordaan, Digby F. Warner, Heinrich C. Hoppe, Dustin Laming, Lesetja J. Legoabe, and Setshaba D. Khanye. Quinolone-isoniazid hybrids: synthesis and preliminary in vitro cytotoxicity and anti-tuberculosis evaluation. Medicinal Chemistry Communications. 2019; 10: 326-331.
39. S. S. Panda, A. Bajwa, R. Ahmad, N. Idrees, E. Yazdani, A. U. Bhat, P. Venkatesan, and U. Meshram, "Design, synthesis and biological evaluation of pyrazinoic acid–isoniazid molecular hybrids," *RSC Advances*, vol. 9, pp. 22608–22618, 2019.

HOW TO CITE: Amerullah Ansari, Sarita, Ankit Kumar Verma, Synthesis, Characterization, Molecular Docking & Evaluation of Antibacterial Activity of Isoniazid-Pyrazole Hybrid Scaffolds, Int. J. of Pharm. Sci., 2026, Vol 4, Issue 6, 6973-6998, https://doi.org/10.5281/zenodo.20958180